Theoretical analysis of thermal effects in fiber laser from the moment when pump is turned on to steady-state

Zilun Chen (陈子伦), Jing Hou (侯 静), and Zongfu Jiang (姜宗福)

Institute of Directed Energy Technology, Photoelectric Science and Engineering School, National University of Defense Technology, Changsha 410073

Received November 7, 2006

A theoretical analysis of the pump-induced temperature change and associated thermal phase shift occurring in a fiber laser is presented. The temperature rise and thermal phase shift from the moment when pump is turned on to steady-state in fiber lasers, such as Yb-doped fiber laser, are numerical calculated. With the same parameters, the numerical solution is in good agreement with the finite-element (ANSYS software) simulation.

OCIS codes: 060.2320, 140.3510, 140.3480, 140.6810.

In the development of fiber lasers, power scaling of ytterbium-doped single-fiber lasers has now led to output power up to 1 kW[1,2]. Potential constraints on power scaling of fiber lasers include thermal effects, optical damage of fiber materials, and nonlinear scattering (especially stimulated Raman scattering)[2]. An alternative approach to building high power lasers is to use relatively lower power laser arrays; however, it requires that the beams from the array elements combined have the propagation characteristics of a single beam. Recently much attention has been paid to coherent combined with master-oscillator power-amplifier (MOPA) architecture[3−5]. But in this architecture, it is the key technology to detect and modulate phase noise in fiber lasers. The phase noise was primarily driven by thermal effects of the doped fiber[6]. Brown and Wang *et al.*[7,8] analyzed steady-state temperature distribution by thermal effects. In this paper, transient temperature distribution and phase shift by thermal effects are analyzed after the pump is turned on.

The goal that we investigate the continuous pumping is to model the temporal evolution of the radial temperature profile and associated thermal phase shift from the time when the pump is turned on. It is assumed to be long enough that the z-dependence of the temperature profile is time invariant, and it is omitted in our notation. The temperature distribution satisfies the heat conduction equation[9]

$$\rho c_v \frac{\partial T(r,t)}{\partial t} - \kappa \nabla^2 T(r,t) = \eta P_v(r), \tag{1}$$

where ρ is the density of the fiber material and c_v its specific heat, fraction η is the absorbed energy turned into heat coefficient, $P_v(r)$ is the average pump power absorbed per unit volume, κ is the thermal conductivity of silica.

For a cylindrically symmetric object such as a fiber, Eq. (1) may be simplified to

$$\frac{\partial T(r,t)}{\partial t} = D\frac{1}{r}\frac{\partial}{\partial r}\left[r\frac{\partial T(r,t)}{\partial r}\right] + \frac{\eta P_v(r)}{\rho c_v}, \tag{2}$$

where $D = \kappa/\rho c_v$ is the thermal diffusivity. The general solution to Eq. (2) is

$$\Delta T(r,t) = \sum_{m=1}^{\infty} a_m J_0\left(\frac{p_m r}{b}\right)\exp\left(-\frac{t}{\tau_m}\right), \tag{3}$$

where $\Delta T(r,t) = T(r,t) - T_0$ is the temperature rise profile, T_0 denotes the equilibrium temperature of the surrounding medium, b is the outer radius of the fiber, and the time constant τ_m is given by

$$\tau_m = \frac{\rho c_v}{\kappa}\frac{b^2}{p_m^2} = \frac{b^2}{D p_m^2}. \tag{4}$$

The coefficients a_m, p_m in Eq. (3) are determined by two boundary conditions. One is energy conversion: assuming that cooling is due to natural air convection, the heat flowing out of the fiber (at $r = b$) is proportional to the temperature difference between the fiber and the surrounding air. The proportionality factor is the heat transfer coefficient h. This condition can be expressed as

$$-\kappa \nabla T(r,t)|_b = h(T(b,t) - T_0). \tag{5}$$

Inserting Eq. (3) into Eq. (5) yields

$$p_m J_1(p_m) = \frac{hb}{\kappa} J_0(p_m), \tag{6}$$

which determines the values of P_m. The other condition is that at $t = 0$, Eq. (2) may be simplified to

$$\frac{\partial T(r,0)}{\partial t} = \frac{\eta P_v(r)}{\rho c_v}. \tag{7}$$

From Eqs. (3) and (7), we can obtain

$$\frac{\partial a_m}{\partial t} = \frac{\eta \int_0^b \frac{P_v(r)}{\rho c_v} J_0(\frac{p_m r}{b}) r \mathrm{d}r}{\frac{b^2}{2} J_0^2(p_m)(1 + (\frac{bh}{\kappa p_m})^2)} \exp(\frac{t}{\tau_m}), \tag{8}$$

with $a_m(t = 0) = 0$.

Equation (8) can be simplified to

$$a_m = \frac{\eta \int_0^b \frac{P_v(r)}{\rho c_v} J_0(\frac{p_m r}{b}) r \mathrm{d}r}{\frac{b^2}{2} J_0^2(p_m)(1 + (\frac{bh}{\kappa p_m})^2)} \tau_m [\exp(\frac{t}{\tau_m}) - 1]. \tag{9}$$

Inserting Eq. (9) into Eq. (3) yields

$$\Delta T(r,t)=\sum_{m=1}^{\infty}\frac{2\eta\int_0^b P_v(r)J_0(\frac{p_m r}{b})r\mathrm{d}r}{kp_m^2J_0^2(p_m)(1+(\frac{bh}{\kappa p_m})^2)}$$

$$\times[1-\exp(-\frac{t}{\tau_m})]J_0(\frac{p_m r}{b}). \quad (10)$$

Heating of the fiber induces a phase change in the signal by two effects, namely, changing the index of refraction ($\delta n/\delta T$) coefficient and longitudinal expansion of the fiber. Since the second contribution amounts to less than 2% of the first one, in this paper we only include the thermal index change[7,9]. The change of the effective index of the signal mode is given by

$$\Delta n=\frac{\partial n}{\partial T}\int_0^b \Delta T(r,t)f_{\mathrm{s}}(r)2\pi r\mathrm{d}r, \quad (11)$$

where $f_{\mathrm{s}}(r)$ is the signal mode intensity (normalized to unit power). The instantaneous thermal phase shift experienced by the signal is obtained by integrating Eq. (11) along z

$$\Delta\phi_{\mathrm{th}}=\frac{2\pi}{\lambda_{\mathrm{s}}}\frac{\partial n}{\partial T}\int_0^l\int_0^b \Delta T(r,t)f_{\mathrm{s}}(r)2\pi r\mathrm{d}r\mathrm{d}z. \quad (12)$$

According to above theory analysis, we get numerical solution for the fiber laser at the Gaussian pumping, where the fiber is pumped with $P_0=100$ W, and $\eta=0.18$, $l=50$ m, other parameters are listed in Table 1.

When the pump is the Gaussian pumping, $P_v(r)$ becomes

$$P_v(r)=\frac{2P_0}{\pi\omega_0^2 l}\exp(-2\frac{r^2}{\omega_0^2}). \quad (13)$$

Inserting Eq. (13) into Eq. (10) yields

$$\Delta T(r,t)=\sum_{m=1}^{\infty}\frac{4\eta P_0\int_0^b \exp(-2\frac{r^2}{\omega_0^2})\,J_0(\frac{p_m r}{b})r\mathrm{d}r}{\pi\omega_0^2 lkp_m^2J_0^2(p_m)(1+(\frac{bh}{\kappa p_m})^2)}$$

$$\times[1-\exp(-\frac{t}{\tau_m})]J_0(\frac{p_m r}{b}). \quad (14)$$

The dopant has a step profile with a radius $s=3$ μm, assuming $\omega_0=s$. From Fig. 1, we can see that shortly after the pump is turned on, the heat and the temperature increasing are mostly confined to the vicinity of the core; as time goes on, the temperature at the center of the fiber increases, and as heat flows outward, the temperature rise spreads toward the edge of the fiber; eventually, the temperature profile becomes nearly uniform. The steady-state temperature rises by 11.4 °C compared with the air temperature.

Table 1. Values of Selected Physical Parameters of a Silica Fiber

Specific Heat c_v	741 J/(kg·K)
Refractive Index n	1.44
Index Temperature Coefficient $\mathrm{d}n/\mathrm{d}T$	1.1×10^{-5} K^{-1}
Thermal Conductivity κ	1.38 W/(m·K)
Thermal Diffusivity D	8.46×10^{-7} m^2/s
Specific Gravity ρ	2.2×10^{3} kg/m^3
Heat Transfer Coefficient h	40.7 W/(m^2·K)

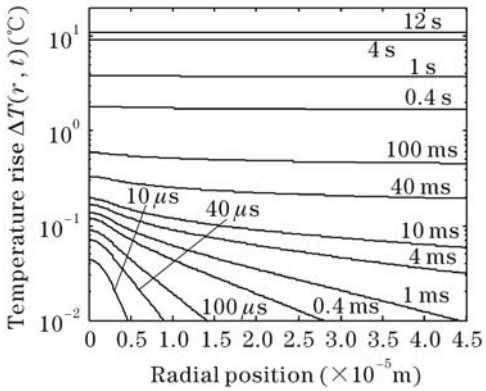

Fig. 1. Radial temperature profile in a fiber at various times, continuously pumped fiber with a step absorption profile of radius $\omega_0=3$ μm.

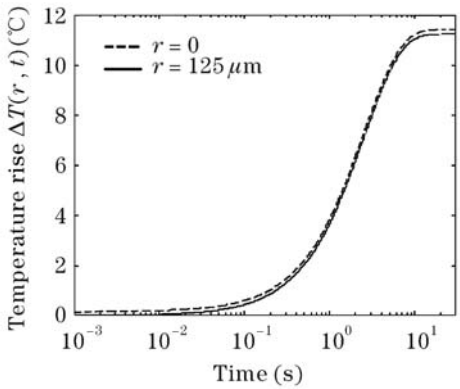

Fig. 2. Temperature rise at the center (dashed line) and edge (solid line) of a continuously pumped fiber with a step absorption profile of radius $\omega_0=3$ μm.

The same data is shown in Fig. 2 in the form of the temporal evolution of the temperature at the center ($r=0$, dashed curve) and edge ($r=125$ μm, solid curve) of the fiber. At both locations, the temperature rises slowly at first (for $t\leq100$ ms), then more rapidly for a few seconds, until finally levels off asymptotically to a steady-state value (about rise by 11.4 °C compared with the air temperature at $r=0$) for 12 s. All the time the temperature rise at the edge of the cladding remains slightly below that at the center of the core.

Assuming that $f_{\mathrm{s}}(r)$ can be approximated by a Gaussian distribution. For the signal mode,

$$f_{\mathrm{s}}(r)=\frac{1}{\pi r_{\mathrm{s}}^2}\exp(-\frac{r^2}{r_{\mathrm{s}}^2}). \quad (15)$$

Equation (11) becomes

$$\Delta\phi_{\mathrm{th}}=\frac{4\pi}{\lambda_{\mathrm{s}}}\frac{l}{r_{\mathrm{s}}^2}\frac{\partial n}{\partial T}\int_0^b \Delta T(r,t)\exp(-\frac{r^2}{r_s^2})r\mathrm{d}r. \quad (16)$$

Inserting the rise temperature into Eq. (15), we can get the time serial of phase shift induced by thermal effects. Figures 3(a) and (b) are the varieties of phase shift and

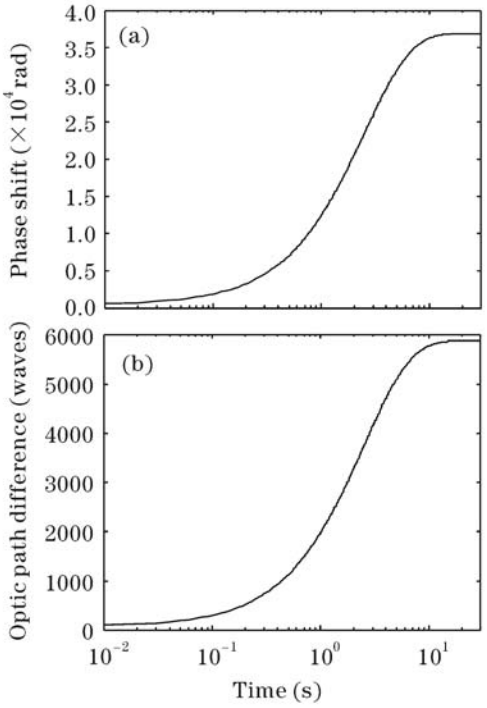

Fig. 3. (a) Phase shift rise and (b) optic path difference rise of a continuously pumped fiber with a step absorption profile of radius $\omega_0 = 3$ μm.

optic path difference induced by thermal effects with time going on, respectively. From the pump turned on to the steady-state, the phase shift is 3.7×10^4 radians, and the optic path difference changes to 5800λ (when $\lambda = 1064$ nm).

Having derived the transient thermal effects in fiber laser by numerical solution, we now turn attention to finite-element simulation by ANSYS software. When the pump is turned on, only a fraction of the absorbed pump power is turned into heat in fiber core. In the finite-element simulation by ANSYS software, we assume that the distribution of heat is Gaussian in fiber core.

Using the same parameters with numerical solution, simulated results with finite-element method (ANSYS software) are shown in Fig. 4. It is the form of the temporal evolution of the temperature at the center ($r = 0$)

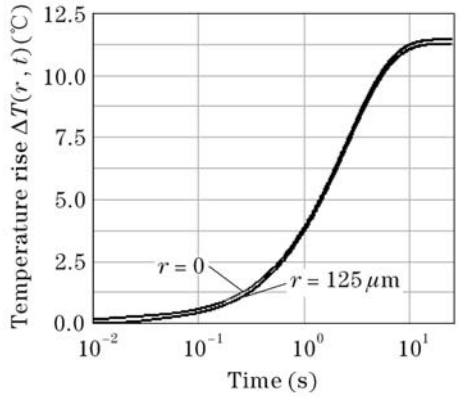

Fig. 4. Temperature rise at the center and edge of a continuously pumped fiber with a step absorption profile of radius $\omega_0 = 3$ μm.

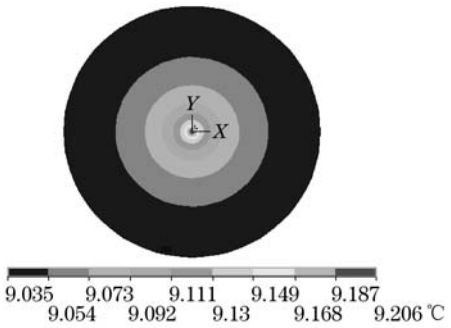

Fig. 5. Temperature distribution at cross section of the doped fiber after the pump has been turned on for 5 seconds.

and edge ($r = 125$ μm) of the fiber. From Figs. 4 and 2, we can see that the results are almost the same as the numerical solution. Figure 5 is the temperature distribution of the fiber cross section after the pump has been turned on for 5 seconds. The temperature at the center and edge of the fiber are 9.035 and 9.206 °C, respectively.

We have presented analysis of the temperature rise and associated thermal phase shift occurring in a fiber laser or fiber amplifier by continuous wave (CW) pumping by using 100-W pump light and 50-m fiber. From the results of the numerical solution and finite-element simulation, it is concluded that the rise time of the fiber temperature is in the range of ten seconds; at steady-state, the temperature is almost uniform across the fiber cross section. When reaching steady-state, the core's temperature rise by 11.4 °C compared with the air temperature, phase shift is almost 3.7×10^4 radians. The numerical solution is in good agreement with the finite-element simulation.

This work was supported by the National Natural Science Foundation for Youth of China (No. 60608008) and the Project of National University of Defense Technology (No. JC05-07-04). Z. Chen's e-mail address is zilun1978@yahoo.com.cn.

References

1. Y. Jeong, J. K. Sahu, D. N. Payne, and J. Nilsson, Opt. Express **12,** 6088 (2004).
2. V. Gapontsev, D. Gapontsev, N. Platonov, O. Shkurikhin, V. Fomin, A. Mashkin, M. Abramov, and S. Ferin, in *Proceedings of Conference on Lasers and Electro-Optics Europe* 508 (2005).
3. J. Anderegg, S. Brosnan, M. Weber, H. Komine, and M. Wickham, Proc. SPIE **4974,** 1 (2003).
4. S. J. Augst, T. Y. Fan, and A. Sanchez, Opt. Lett. **29,** 474 (2004).
5. T. Y. Fan, IEEE J. Sel. Top. Quantum Electron. **11,** 567 (2005).
6. B. He, Q. Lou, J. Zhou, D. Xue, J. Dong, Y. Wei, Y. Qi, and Z. Wang, Chin. J. Lasers (in Chinese) **33,** 1153 (2006).
7. D. C. Brown and H. J. Hoffman, IEEE J. Quantum Electron. **37,** 207 (2001).
8. Y. Wang, C. Q. Xu, and H. Po, IEEE Photon. Technol. Lett. **16,** 63 (2004).
9. M. K. Davis, M. J. F. Digonnet, and R. H. Pantell, J. Lightwave Technol. **16,** 1013 (1998).